PHYSICAL REVIEW B VOLUME 8, NUMBER 3 1 AUGUST 1973

# Multiphonon Relaxation of Excited States of Rare-Earth Ions in $YVO_4$, $YAsO_4$, and $YPO_4$ †

Edward D. Reed, Jr. and H. Warren Moos
*Department of Physics, The Johns Hopkins University, Baltimore, Maryland 21218*
(Received 29 January 1973)

The multiphonon relaxation process has been studied in the host crystals $YVO_4$, $YAsO_4$, and $YPO_4$ using the rare earths $Ho^{3+}$, $Er^{3+}$, $Eu^{3+}$, and $Pr^{3+}$ as probes. Lifetimes were measured with the phase-shift technique using a high-frequency (60-kHz maximum) mechanical light chopper of new design. Measurements were made of the multiphonon relaxation rate at 4.2 °K on many of the rare-earth $J$ manifolds, and of the temperature dependence of the rate for selected manifolds. Vibronic sidebands were recorded for $YVO_4$ and $YAsO_4$. Both the 4.2 °K multiphonon decay rate as a function of energy gap to the next lower manifold and the temperature dependences of these rates indicate that individual peaks in the phonon energy distribution (as determined from the vibronics) play a strong role in the decay, in contrast to previous results.

## I. INTRODUCTION

When an upper level of a rare-earth ion in a crystal is excited, it may decay by radiating, by an ion-pair process, or by the emission of several phonons. The last process is the subject of this paper.[1] Multiphonon (MP) relaxation occurs from the excited $J$ manifold (a $J$ manifold is a set of energy levels, each of which is characterized by the same value of total angular momentum $J$) to the next manifold below, so that an energy of perhaps several thousand $cm^{-1}$ is required to be taken up by the lattice. Thus, the number of phonons required depends on the energy gap between the two manifolds and on the phonon spectrum of the host crystal. MP relaxation is usually studied by determining transition rates for the process. Total transition rates (i.e., reciprocals of the fluorescence lifetimes) are measured and the MP decay rates are extracted from these. Weber determined them for several ions in $LaF_3$[2,3] and $Y_2O_3$[4] by subtracting from the measured total transition rates the calculated radiative transition rates. Partlow and Moos[5] developed a technique for measuring MP relaxation quantum efficiencies (the fraction of the ions which decay by MP decay) which they used to determine MP transition rates for $Nd^{3+}$ in $LaCl_3$. Riseberg, Gandrud, and Moos[6] later used this technique with the low-lying manifolds of $LaCl_3:Dy^{3+}$. Riseberg and Moos[7] carried out a systematic study of MP relaxation in the lattices $LaBr_3$, $LaF_3$, $SrF_2$, and $Y_2O_3$.

$YVO_4$, $YAsO_4$, and $YPO_4$ all have the same tetragonal structure (space group $D_{4h}^{19}$). Raman and infrared spectra of $YVO_4$[8] and $YPO_4$[9,10] indicate that their phonon energy distributions extend to about 900–1000 $cm^{-1}$ and that there is a gap in the phonon spectra in the approximate range 500–800 $cm^{-1}$. Furthermore, the very-high-energy optical phonons derive from internal vibrations of the $XO_4$ ($X$ = V or P) complex, which may interact with the rare-earth ions differently from the low-energy phonons. By contrast, the phonon spectra of the lattices studied previously extended to a few hundred $cm^{-1}$ (e.g., 175 $cm^{-1}$ for $LaBr_3$ and 260 $cm^{-1}$ for $LaCl_3$) with no gaps, and there were no molecular complexes. The lattices used in this study thus seemed like good candidates for revealing some different aspects of the MP relaxation process.

In Sec. II the phenomenological model of the MP process is discussed briefly. The experimental details are discussed in Sec. III, and the experimental results in Sec. IV. The results consist of a report and discussion of the MP transition rates (measured at 4.2 °K) for several manifolds plotted against energy gap to the next lower manifold for each of the three hosts, the temperature dependences of the MP transition rates of several manifolds in $YVO_4$ and $YAsO_4$, and vibronic sideband spectra for $YVO_4$ and $YAsO_4$. In the following paper[11] we discuss the results on $Eu^5D_1$ in $YVO_4$, and, briefly, the results on $Ho\,E(^5S_2, {}^5F_4)$ in $YVO_4$ and $YAsO_4$. In these cases MP relaxation at 4.2 °K was occurring from a *nonthermalized* manifold.

## II. BACKGROUND

The isolated rare-earth ion can be thought of as interacting with its crystalline environment via the crystal field, which is time varying because the lattice is vibrating.[12] The interaction Hamiltonian can be written[7]

$$H_{\text{xtal}} = V_0 + \sum_i V_i Q_i + \frac{1}{2}\sum_{i,j} V_{ij} Q_i Q_j + \cdots . \qquad (1)$$

$V_0$ is the interaction with the static crystal field and the remaining terms, involving the normal coordinates $Q_i$, represent the interaction with the vibrating lattice. While the use of such an expression for making calculations is hampered by a lack of knowledge of several of the quantities

involved, it serves as a basis for a phenomenological model of the $p$-phonon process. A transition between two electronic states accompanied by the emission or absorption of $p$ phonons can be viewed theoretically by using the second term in Eq. (1) in $p$th-order time-dependent perturbation theory. Alternatively, the $(p+1)$th term (involving $p$ $Q_i$'s) in Eq. (1) can be used in first-order perturbation theory. The expression for $W^{(p)}$, the transition rate involving the emission of $p$ phonons, when both mechanisms are included has been presented elsewhere.[7] It predicts that the temperature dependence of the MP transition rate has the form

$$W^{(p)} = W_0 \prod_i (n_i+1)^{p_i} \quad . \tag{2}$$

Here $p_i$ is the number of phonons emitted with energy $\hbar\omega_i$, so that $\sum_i p_i = p$. $W_0$ is the transition rate for the decay at $T=0\,^\circ$K, and $n_i$ is the Bose-Einstein occupation probability

$$n_i = [e^{\hbar\omega_i/kT} - 1]^{-1} \tag{3}$$

The 1 in the parentheses of Eq. (2) represents the spontaneous emission of phonons and the $n_i$ the emission stimulated by thermal phonons. If $\Delta E$ is the energy gap, there is also the constraint

$$\sum_i p_i \hbar\omega_i = \Delta E \quad . \tag{4}$$

In practice, one does not observe the MP transition rate between two energy levels, but that between two $J$ manifolds. The MP transition rate of each level in the upper manifold is the sum of the rates to each level in the lower manifold. Also, the MP transition rate of the upper manifold will be a weighted sum (according to the relative populations) of the rates for each level in the upper manifold. Let $W_i$ be the MP transition rate of the $i$th level and $g_i$ its degeneracy. Assuming that the transition rates between the levels of the manifold are much greater than the $W_i$ (as will be shown elsewhere,[11] this assumption of rapid thermalization is not always valid), the MP transition rate of the manifold is

$$W = \sum_i W_i g_i e^{-\Delta_i/kT} \Big/ \sum_i g_i e^{-\Delta_i kT} \quad , \tag{5}$$

where the sum is over the levels of the manifold and $\Delta_i$ is the energy separation of the $i$th level and the lowest in the manifold.

This phenomenological theory has been used to explain the temperature dependences of the MP transition rates observed in several host crystals.[5-7] It was possible to fit the particular manifold using phonons of a single energy, so that Eq. (2) became $W^{(p)} = W_0\,(n+1)^p$ and $p\hbar\omega = \Delta E$. Application of Eq. (5) was greatly simplified by assuming only one or two nondecaying ($W_i = 0$) levels above the lowest in the manifold; $g_i$, $\Delta_i$, and $W_1$ (1 designates the lowest level) were then adjusted for a best fit to the data. The temperature dependence of $W_1$ is contained in the factor $(n+1)^p$. The fits yielded an order $p$ for the MP process. Now for each lattice studied the highest-energy optical phonons $\hbar\omega_{\max}$ were known from vibronic sideband spectra. In each lattice the order $p$ of the MP transition rate was found to obey the relation

$$p \approx \Delta E/\hbar\omega_{\max} \quad . \tag{6}$$

Thus, the relaxation was observed to occur by emitting the smallest number of phonons consistent with the energy gap and the cutoff in the lattice phonon spectrum. When the 4.2 °K MP transition rates of several manifolds were plotted against $\Delta E$ for a particular host crystal, they were found to follow closely the relation

$$W = C e^{-\alpha \Delta E} \quad , \tag{7}$$

where $C$ and $\alpha$ are positive constants characteristic of the particular crystal. Using Eq. (6), the low-temperature transition rate was seen to decrease exponentially with order $p$. To summarize, it was concluded that the MP decay involved high-energy optical phonons and occurred in the lowest order possible consistent with energy conservation and the cutoff in the phonon spectrum. The observed exponential dependence of the MP relaxation rate on energy gap, independent of the rare-earth manifold involved, was interpreted as being due to the statistical averaging out of the exact features of the interacting phonon modes and ion levels. The results of Sec. IV indicate a more complex behavior in the more complicated systems with molecular groups reported here.

The only selection rule which has been observed in MP relaxation manifests itself when the two manifolds involved have $J=0$ and $J=1$. Weber[2] noted it in the $^5D_1 \rightarrow {}^5D_0$ relaxation of $Eu^{3+}$ in $LaF_3$ and Kiel[13,14] in the $^3P_1 \rightarrow {}^3P_0$ decay of $Pr^{3+}$ in $LaCl_3$. These decays were also found to be abnormally slow (for their energy gaps) in the host crystals of this study.

More recently, a new theoretical approach to the problem of MP relaxation of rare-earth ions in crystals has been discussed by Fong, Naberhuis, and Miller.[15] They considered two electronic states and derived an expression for the MP transition rate which depended explicitly on the electronic energy gap, the temperature, and the phonon energy. The derivation did not take into account any sharp variations in the phonon density of states with energy. Such a theory does not appear to be directly applicable in the present study since, as will be seen, the variations in the phonon density of states play a major role in determining MP relaxation rates.

### III. EXPERIMENTAL TECHNIQUES

All of the crystals used in this study were grown in this laboratory using a flux method due to Feigelson.[16] The $Y_2O_3$ used in this process was stated by the manufacturer to be 99.9999% pure with respect to other rare earths. The dopant oxides were 99.999% pure with respect to other rare earths. The dopant concentration was always 1 at.% or less. Samples were grown in quantities which yielded about $\frac{1}{2}$ g of many small crystals, each typically $5\times\frac{1}{2}\times\frac{1}{2}$ mm in size. The $\frac{1}{2}$ g of crystals was then encapsulated in a quartz tube under about $\frac{1}{2}$ atm of He. Standard techniques, using pumped-on liquid He, cold He and $N_2$ gases, and an oven, were used to control the sample temperature.

The spectroscopic techniques used were standard and are reported in a number of previous papers.[1] Fluorescence lifetimes were measured using the phase-shift method, in which one measures the phase shift $\phi$ between the first Fourier components of the chopped pump light and the fluorescence. The lifetime $\tau$ is then calculated from

$$W \equiv 1/\tau = 2\pi f/\tan\phi \quad , \tag{8}$$

where $f$ is the chopping frequency.[17] $W$ is the total transition rate. Exponentiality of the fluorescence decay was checked by measuring $W$ at several different chopping frequencies.

A block diagram of the apparatus used for measuring lifetimes is shown in Fig. 1. Light from the premonochromator was collimated before entering the light chopper. The motor and chopping wheel were mounted in a vacuum to eliminate air friction and allow the motor to reach its maximum speed of 10 000 rpm. The motor and feedback electronics for controlling its speed were those of Opal and Gandrud.[18] Chopper frequency stability was excellent; frequency drift was never a problem in the phase-shift measurements. The fluorescence was focused onto the entrance slit of a 0.3-m Czerny-Turner spectrometer. Interference and Corning glass filters were used in the pump and fluorescence beams to reduce scattered light and grating orders. Light was detected with *S*20 and *S*1 photomultipliers and an InAs infrared detector.

While the conventional type of mechanical chopper consists simply of a rotating wheel with radial slots (slots cut along a radius) or holes spaced uniformly along its circumference, this one operated quite differently. It used a rotating wheel with very fine radial slots in it (wheels with 180 and 360 slots were used) and, in addition, another piece of the wheel material with identical slots in it which was kept stationary. This stationary piece was located about $\frac{1}{8}$ in. from the wheel along the direction of the light beam. The slots in the wheel (and stationary piece) were cut so that they were approximately the same width as the material between slots. As the wheel rotated, 50% of the light beam (having a diameter of about 1.5 in.) was transmitted when the slots in the two sets (rotating and stationary) covered each other, and was blocked when the material between slots in one set covered the slots in the other. This chopper had two distinct advantages over the conventional chopper. First, since the light beam was broad and passed through many slots at once, the slot width could be made as small as possible in order to obtain high chopping rates (necessary for measuring short lifetimes). In fact, much higher frequencies than the 60 kHz attained are practicable. Second, since a collimated beam was chopped, there was little phase variation over the image of the chopped pump light at the sample. This is necessary when doing phase-shift measurements because the pump light must have a well-defined phase in order to accurately determine the phase shift of the fluorescence.

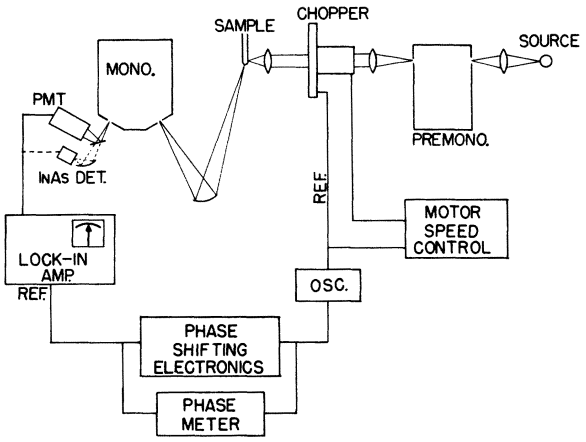


FIG. 1. Apparatus used for measuring fluorescence lifetimes.

Phase shifts were measured using a PAR model No. HR-8 lock-in amplifier in conjunction with an external phase shifting and measuring network. The external network was required because the internal phase shifter of our HR-8 was found to be unreliable above about 5 kHz. A phase shift variable from 0° to about 120° was introduced into the reference signal using a shifter which kept the signal level approximately constant as the phase shift was varied. The resulting phase shift was measured using a Wiltron model No. 351 phase meter. The oscillator in Fig. 1 converted the square wave chopper reference signal into the sine wave required by the Wiltron.

The reciprocal of the measured fluorescence lifetime gives the total transition rate, i.e., the

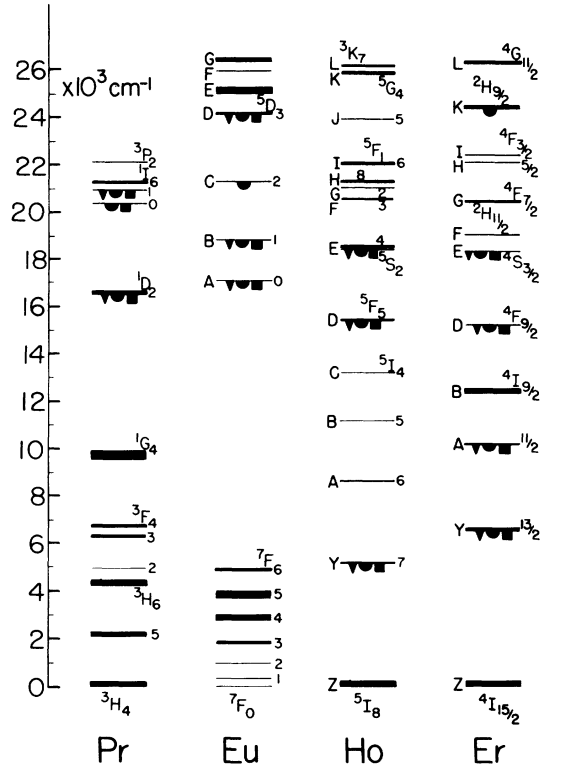


FIG. 2. Fluorescent $J$ manifolds (at 4.2 °K) of the triply ionized rare earths in $YVO_4$, $YAsO_4$, and $YPO_4$. A triangle, half-circle, or square under a manifold means that it was observed to fluoresce in the host $YVO_4$, $YAsO_4$, or $YPO_4$, respectively. The widths shown for the manifolds are those in $LaCl_3$ (see Ref. 21).

sum of the rates due to all processes which deplete the manifold. These include migration to sinks, ion-pair decay, MP relaxation, and radiative decay. Migration to sinks could be eliminated as a possible decay mechanism because of the low rare-earth impurity concentration used.[19] A resonant ion-pair decay was generally not energetically possible for the rare-earth manifolds studied; if it appeared possible, fluorescence spectra could be obtained, in all but four cases (noted later), which showed that it was not occurring. Nonresonant ion-pair decay was not investigated and was assumed to be negligible. Fluorescence intensities showed, in all cases to be discussed, that the lifetimes of the manifolds were determined almost completely (MP relaxation quantum efficiencies $\geq$ 90%) by the MP relaxation process. Thus the MP relaxation rates reported are essentially the reciprocals of the measured fluorescence lifetimes, with only minor corrections for the radiative decay contributions.

## IV. EXPERIMENTAL RESULTS

Figure 2 shows the manifolds in the four rare earths studied which were observed to fluoresce. Manifolds with energy gaps $\lesssim$ 2500 $cm^{-1}$ do not generally fluoresce. With Ho and Er, manifolds up to 28 000 $cm^{-1}$ were excited, but in only one instance (Er $K$ in $YAsO_4$) was fluorescence observed from a manifold above 20 000 $cm^{-1}$. Except for Pr $^1D_2$ and Eu $^5D_0$, the fluorescences in $YPO_4$ were much weaker than those in $YVO_4$ and $YAsO_4$ (which were of comparable magnitude). This is probably due to a tighter coupling between the ions and lattice

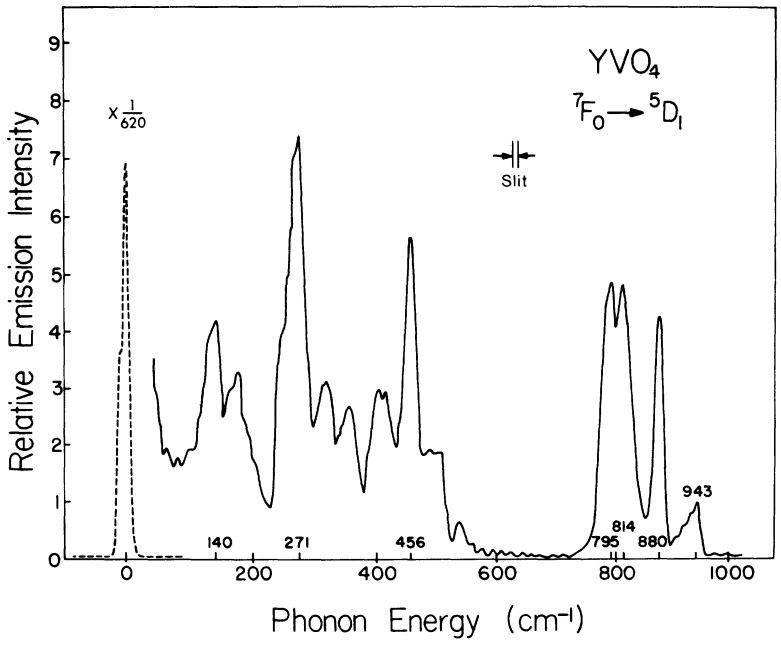


FIG. 3. Vibronic spectrum of Eu $^5D_1$ in $YVO_4$. This was recorded as an excitation spectrum at 77 °K, monitoring the $^5D_0 \rightarrow {}^7F_2$ fluorescence. The electronic transitions are shown in dashes.

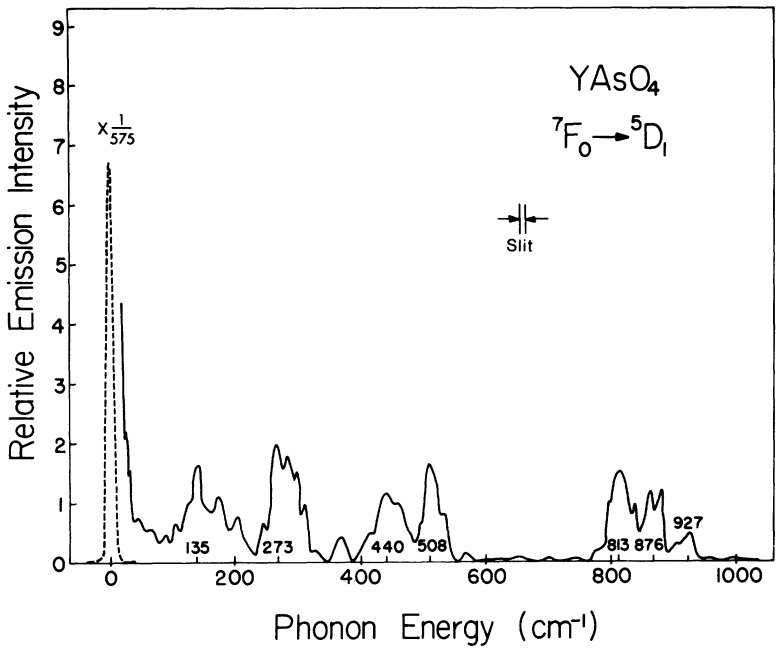


FIG. 4. Vibronic spectrum of Eu $^5D_1$ in $YAsO_4$, recorded as in Fig. 3.

vibrations in $YPO_4$. The fluorescences were so weak in $YPO_4$ that no lifetimes could be followed to temperatures above 4.2 °K, since the fluorescence intensity generally decreased at higher temperatures. The fact that Pr $^3P_1$ fluoresces at all is understandable in terms of the $J=1 \rightarrow J=0$ selection rule.

Figures 3 and 4 show the vibronic sidebands of $YVO_4$ and $YAsO_4$. These will be used in the interpretation of the MP transition-rate temperature dependences in these hosts. They were recorded at 77 °K as excitation spectra, pumping the Eu $^5D_1$ manifold while monitoring the very bright $^5D_0 \rightarrow {}^7F_2$ fluorescence. Owing to the close spacings of the two $^5D_1$ Stark levels (9 $cm^{-1}$ in $YVO_4$ and about 5 $cm^{-1}$ in $YAsO_4$), the associated vibronics reflect with only slight ambiguity the energies of the phonon states. Note the narrow widths of some of the vibronic peaks, particularly those beyond about 800 $cm^{-1}$. An interesting feature of these spectra is the gap in the available phonons between about 500 and 800 $cm^{-1}$. These gaps and the sharpness of the peaks in the distributions of phonons in energy (assuming the vibronic spectrum of each host crystal is representative of its relative energy distribution of phonons[20]) had a dramatic effect on the MP relaxation rates. Many of the vibronic peaks in $YVO_4$ are energetically close to previously observed Raman and infrared lines.[8] The vibronic spectrum of $YPO_4$ is not shown because it is not needed in a discussion of MP transition-rate temperature dependences. It is similar to those of $YVO_4$ and YAsO4, but much weaker. (It could not be seen in an excitation spectrum pumping $^5D_1$, and was very weak in a $^5D_2$ excitation spectrum.)

Figures 5 – 7 show the results of plotting the MP relaxation rates ($W_{mp}$) measured at 4.2 °K against the energy gaps of the next lower manifolds. The gaps were determined from the energy levels in $LaCl_3$[21] and were taken to be the energy separation

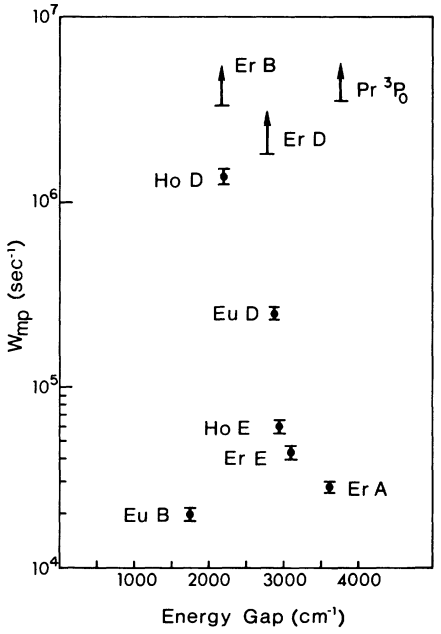


FIG. 5. Energy-gap dependence of the 4.2 °K MP transition rate in $YVO_4$. The possibility of a resonant ion-pair process contributing to the decay of Eu $D(^5D_3)$ cannot be ruled out.

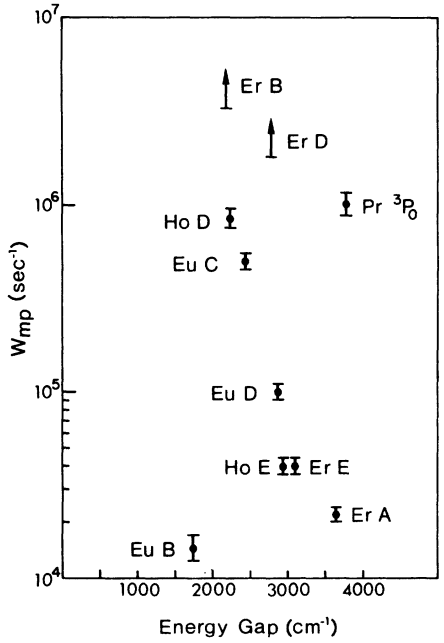


FIG. 6. Energy-gap dependence of the 4.2 °K MP transition rate in $YAsO_4$. The possibility of a resonant ion-pair process contributing to the decay of Eu $D(^5D_3)$ cannot be ruled out.

of the lowest level in the manifold of interest and the middle of the next-lower manifold. While the relaxation rates show a general upward trend as the gap decreases, the scatter is too great to fit the data to a functional form such as Eq. (7). An order for the MP process can be determined for each manifold whose $W_{mp}$ was followed to high temperatures (see below). If, as in Refs. 6 and 7, the 4.2 °K relaxation rates are plotted against these orders (not shown), even more scatter of the data points is obtained than in Figs. 5 and 6. This scatter can be explained by the large, sharp variations in the phonon energy distributions, as shown in the vibronic spectra. A small change in the energy gap can bring into play a quite different density of phonon states available to the transition. This could act in two ways to produce the scatter of data points in a decay-rate–versus–order plot. First, it could cause large variations in the rates among relaxations which occur by the same order. Second, it could cause to be erroneous the assignment of an order to the 4.2 °K relaxation using the high-temperature relaxation rates. This is because higher Stark levels are populated at elevated temperatures, and these could decay via a different-order MP process than the lowest level in the manifold. The large MP relaxation rates in $YPO_4$ account for the generally much weaker fluorescences in this host. The slowness of the Eu $B(^5D_1)$ decay in all three hosts can be explained by the $J = 1 \rightarrow J = 0$ selection rule.

In attempting to fit the MP transition-rate temperature dependences in $YAsO_4$ and $YVO_4$, the stimulated-phonon-emission model of Eq. (2) was used. In order to obtain a reasonable fit to the data for a given manifold, it was usually necessary that phonons of different energies be used. Furthermore, an attempt was made to use only phonons with energies close to those of the peaks in the vibronic spectrum for the lattice. The simplest model (all phonons of the same energy) was tried first. If this did not explain the data a more complicated combination of phonons was tried. A constraint on the fitting was, of course, that the sum of the phonon energies approximately equal the energy gap. With a given gap and a given order for the MP process, making all phonons the same energy resulted in the slowest predicted rate of increase of $W_{mp}$ with temperature. Increasing the energy of one phonon while decreasing that of another, subject to the gap constraint, caused the predicted rate-versus-temperature curve to rise faster as the temperature was increased. Increasing the order of the model caused the predicted curve to rise much faster with increasing temperature. Finally, no attempt was made to fit the very-low-temperature data since they are strongly influenced by thermal population of higher Stark levels of the manifold.

As an example of the observed MP transition

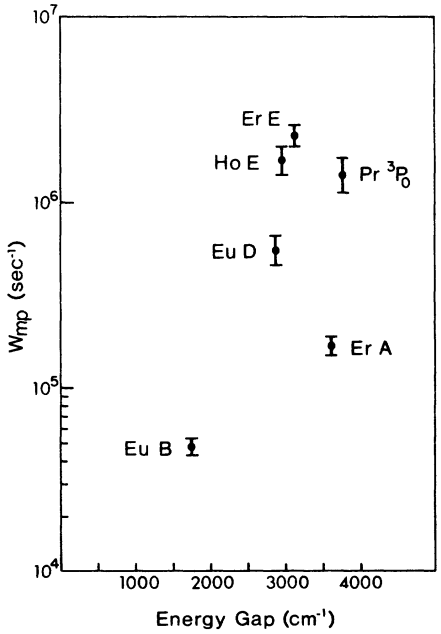


FIG. 7. Energy-gap dependence of the 4.2 °K MP transition rate in $YPO_4$. The possibility of a resonant ion-pair process contributing to the decays of Ho $E(^5S_2, ^5F_4)$ and Eu $D(^5D_3)$ cannot be ruled out.

rates as a function of temperature, Fig. 8 shows Er $E(^4S_{3/2})$ in $YVO_4$. The error bar shown on each data point indicates the absolute error for it; the relative error between points is much less than this, as can be seen from the smoothness of the data. Er $E$ contains four states and its energy gap is nominally 3100 $cm^{-1}$. Er $F(^2H_{1-1/2})$, containing twelve states, lies about 700 $cm^{-1}$ above it. This is important because Er $E$ can be significantly depopulated by Er $F$ at high temperatures. Another point to note is that the Stark splitting of Er $E$ is very small. (As would be expected in $D_{2d}$ symmetry, only two absorption lines were seen in the low-temperature spectrum of Er $E$, split about 5 $cm^{-1}$). As shown in Fig. 8, at very low temperatures there appears to be a small increase in $W_{mp}$ with temperature due to thermal population of the higher-$E$ Stark level. The data above 50° K are fit quite well by the function

$$W_{mp} = 5.00\times10^4 \frac{[n(270)+1]^2[n(880)+1]^3}{1+3\,e^{-700/kT}}\ \text{sec}^{-1}, \quad (9)$$

where the notation $n(270)$ means the phonon-mode occupation probability [Eq. (3)] evaluated at $\hbar w_i = 270\ cm^{-1}$. This was derived from Eq. (5) with $W_i$ taken to be 0 for all states in $F$ and $W_i = 5.00\times10^4[n(270)+1]^2[n(880)+1]^3\ \text{sec}^{-1}$ for each of the four $E$ states. This last expression represents the emission of two 270-$cm^{-1}$ and three 800-$cm^{-1}$ phonons. The low-energy phonons are necessary to explain the rapid rise in $W_{mp}$ as the temperature increases between 100 and 300 °K. Because of the narrow energy spread of the Er $E$ levels, there could not be any significant increase in $W_{mp}$ above 100 °K due to thermal population within Er $E$. The gap in the energies of the phonon states in $YVO_4$ appears to have forced the use of two phonons of small energy (whose energy sum lies in the gap). (As can be seen from Table I, this feature is also exhibited by the data for Er $E$ in $YAsO_4$). For comparison, the fit provided by the simple model of Riseberg and Moos[7] is shown by a dashed line in Fig. 8. Its analytic form is

$$W_{mp} = 5.00\times10^4 \frac{[n(517)+1]^6}{1+3\,e^{-700/kT}}\ \text{sec}^{-1}. \quad (10)$$

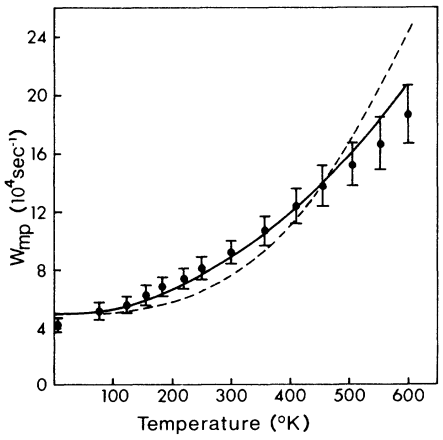


FIG. 8. MP transition-rate temperature dependence of Er $E(^4S_{3/2})$ in $YVO_4$. The solid line is the dependence expected from the emission of two 270-$cm^{-1}$ and three 880-$cm^{-1}$ phonons from the four states of Er $E$, along with depopulation to a nondecaying $F(^1H_{11/2})$ manifold 700 $cm^{-1}$ above. See Eq. (9). The dashed line shows the prediction of the simpler model which uses equal-energy phonons. See Eq. (10). The relative error between data points is much less than the absolute error indicated by the error bars.

TABLE I. Analytic expressions which fit the observed MP transition-rate temperature dependences for additional manifolds.

| Manifold | Lattice | $W_{mp}(\text{sec}^{-1})$ |
|---|---|---|
| Er $A$ | $YVO_4$ | $4.00\times10^4[n(880)+1]^4$ |
| | $YAsO_4$ | $1.70\times10^4\{[n(812)+1]^3[n(510)+1]^2+[n(875)+1]^4\}$ |
| Er $E$ | $YAsO_4$ | $3.30\times10^4\,\frac{[n(440)+1]\,[n(250)+1]\,[n(812)+1]^3}{1+3e^{-700/kT}}$ |
| Ho $D$ | $YVO_4$ | $2.50\times10^5\,[n(880)+1][n(450)+1]^3 + 9.50\times10^5[n(880)+1]^2[n(450)+1]$ |
| | $YAsO_4$ | $2.00\times10^5[n(440)+1]^3[n(880)+1] + 7.20\times10^5[n(880)+1]^2[n(440)+1]$ |

$W_{mp}$ temperature dependences were also measured for several other manifolds. These data plots are not shown (they are shown in Ref. 1), but the analytic expressions which fit the data are listed in Table I. As above, the coupling strengths of the high- and low-energy phonons with the rare-earth ion were assumed the same. These generally provided slightly better fits than the one shown in Fig. 8. As shown in Table I, it was sometimes necessary to invoke a model which was a weighted average of two different-order processes. While these results show that relatively simple models can explain the $W_{mp}$ temperature dependences, it cannot be definitely concluded that the decays occur only by these phonon processes. It is quite possible that the decays are more complicated than these models indicate.

## V. SUMMARY AND CONCLUSIONS

The fluorescences of rare-earth ions in $YVO_4$, $YAsO_4$, and $YPO_4$ are generally weak. Manifolds with energy gaps $\lesssim 2500\ cm^{-1}$ do not generally fluoresce. Fluorescences in $YVO_4$ and $YAsO_4$ were observed to be of comparable brightness, while those in $YPO_4$ were considerably weaker. Increasing the temperature usually reduced the fluorescence intensity, with the result that no lifetime measurements could be performed above 4.2 °K for $YPO_4$.

Vibronic spectra were recorded in order to get

an idea of the phonon energy distribution in each lattice, which is useful in the interpretation of MP transition-rate temperature dependences. The vibronics of $YVO_4$ and $YAsO_4$ extend to about 900 $cm^{-1}$, have large variations in magnitude, and vanish between about 500 and 800 $cm^{-1}$. The $YPO_4$ vibronics are similar. These properties appear to significantly affect the MP relaxation rates.

$W_{mp}$ temperature dependences were fit only at high temperatures, using a stimulated-phonon-emission model. The data could usually only be fit with a model which used a sum of phonons of different energies, where the energy of each phonon was that of a peak in the vibronic spectrum for the lattice. In some cases a weighted average of two such models (the two were always of different orders) was required to fit the data. It can be concluded from the $W_{mp}$-versus-temperature data that the order of the process is not the overriding factor in determining the MP relaxation rate in those host crystals. Instead, the entire distribution of phonons in energy must be considered, not just its cutoff energy. This feature emerges in this study because of the sharp variations in the phonon distributions and, in particular, because of the gap in the energies of the phonon states. The effect of the gap appears particularly evident in the $W_{mp}$ temperature dependence for Er $E$ in $YVO_4$. To fit the data, a model was required which used two small phonons whose energy sum lay in the gap. The data for Er $E$ in $YAsO_4$ also exhibited this feature. The idea was raised in the Introduction that the very-high-energy phonons might interact with the rare-earth ions differently from the low-energy phonons; it could not be shown from the data that this is so.

The $W_{mp}$–versus–manifold-energy-gap data are consistent with the above conclusions drawn from the $W_{mp}$-versus-temperature data. The measured MP transition rates (at 4.2 °K) as a function of energy gap show that they do not depend in a simple way on energy gap. Further evidence for the importance of the shape of the phonon energy distribution will be given in the following paper.[11]

---

†Supported by the U.S. Army Research Office, Durham, N. C.

*Visiting Fellow, 1972–1973, Joint Institute for Laboratory Astrophysics—Laboratory for Atmospheric and Space Physics, University of Colorado, Boulder, Colo. 80302

[1]Based on Ph.D. dissertation submitted by Edward D. Reed, Jr. to The Johns Hopkins University, 1972 (unpublished). Available from University Microfilms, Ann Arbor, Mich. For further details see the dissertation.

[2]M. J. Weber, in *Optical Properties of Ions in Crystals*, edited by H. M. Crosswhite and H. W. Moos (Interscience, New York, 1967), p. 467.

[3]M. J. Weber, Phys. Rev. **156,** 231 (1967); Phys. Rev. **157,** 262 (1967).

[4]M. J. Weber, Phys. Rev. **171,** 283 (1968).

[5]W. D. Partlow and H. W. Moos, Phys. Rev. **157,** 252 (1967).

[6]L. A. Riseberg, W. B. Gandrud, and H. W. Moos, Phys. Rev. **159,** 262 (1967).

[7]L. A. Riseberg and H. W. Moos, Phys. Rev. **174,** 429 (1968).

[8]S. A. Miller, H. H. Caspers, and H. E. Rast, Phys. Rev. **168,** 964 (1968).

[9]I. Richman, J. Opt. Soc. Am. **56,** 1589 (1966).

[10]R. W. Mooney and S. Z. Toma, J. Chem. Phys. **46,** 3364 (1967).

[11]Edward D. Reed, Jr. and H. W. Moos, following paper, Phys. Rev. B 8, 988 (1973).

[12]For a brief review of rare-earth relaxation processes see H. W. Moos, J. Lumin. **1,** 106 (1971).

[13]A. Kiel, dissertation (The Johns Hopkins University, 1962) (unpublished).

[14]A. Kiel, in *Quantum Electronics*, edited by P. Grivet and N. Bloembergen (Columbia U.P., New York, 1964), Vol. 1, p. 765.

[15]F. K. Fong, S. L. Naberhuis, and M. M. Miller, J. Chem. Phys. **56,** 4020 (1972).

[16]R. S. Feigelson, J. Am. Ceram. Soc. **51,** 538 (1968); J. Am. Ceram. Soc. **50,** 433 (1967); J. Am. Ceram. Soc. **47,** 257 (1964).

[17]E. A. Bailey, Jr. and G. K. Rollefson, J. Chem. Phys. **21,** 1315 (1953).

[18]C. Opal and W. B. Gandrud, Rev. Sci. Instrum. **38,** 838 (1967).

[19]W. B. Gandrud and H. W. Moos, J. Chem. Phys. **49,** 2170 (1968).

[20]E. Cohen, L. A. Riseberg, and H. W. Moos, Phys. Rev. **175,** 521 (1968).

[21]Gerhard H. Dieke, in *Spectra and Energy Levels of Rare Earth Ions in Crystals*, edited by H. M. Crosswhite and Hannah Crosswhite (Interscience, New York, 1968).